

# Free-standing microstructures of $\text{YBa}_2\text{Cu}_3\text{O}_{7-\delta}$ : A high-temperature superconducting air bridge

L. P. Lee, M. J. Burns, and K. Char  
*Conductus, Inc., Sunnyvale, California 94086*

(Received 22 June 1992; accepted for publication 24 September 1992)

We describe the fabrication of a free-standing  $\text{YBa}_2\text{Cu}_3\text{O}_{7-\delta}$  air bridge for useful applications of microstructures and microcircuits integration. We have used a sacrificial dielectric layer, which was subsequently etched, to produce the air gap between top and bottom layers. We have used conventional photolithographic processing, ion-beam dry etching, and selective wet etching with HF to create the novel microstructures. Step coverage of epitaxial bridge layers have been achieved without significant degradation of the superconducting properties of  $\text{YBa}_2\text{Cu}_3\text{O}_{7-\delta}$  layers.

Silicon microelectromechanical technology is rapidly evolving and a number of innovative fabrication techniques have recently been developed for micromotors and other articulated microstructures.<sup>1</sup> Surface micromachining is based on depositing and etching structural and sacrificial films. After deposition of the films, the sacrificial material is etched away leaving a completely assembled micromechanical structure. For the case of polysilicon films, considerable work has been done over the last several years to demonstrate for specific applications of microstructures.<sup>1</sup> However, the creation of a high-temperature superconductor (HTS) microstructure technology requires different techniques and epitaxial multilayer structures which are intrinsically different from conventional Si micromachining technology. This is because HTS microstructures need to be built from an entirely epitaxial technology,<sup>2</sup> in which successive layers must be highly aligned in both the growth direction and in plane. The  $\text{YBa}_2\text{Cu}_3\text{O}_{7-\delta}$  (YBCO) air-bridge technique described in this letter can be extended to make YBCO membrane structures for detectors<sup>3</sup> and micromachines.

In this letter, we describe the fabrication of a free-standing YBCO air bridge that can be used in microstructures and microcircuits integration. These structures are fabricated with conventional photolithographic processing, ion-beam dry etching, and selective wet etching with a HF solution.<sup>4</sup> The films are grown by laser deposition on either  $\text{LaAlO}_3$  or yttria-stabilized zirconia (YSZ) substrates. More detailed process conditions for epitaxial film growth are described in Ref. 2.

A YBCO air bridge fabricated on a  $\text{LaAlO}_3$  substrate is shown in Fig. 1. This 10- $\mu\text{m}$ -wide air bridge was grown over a sacrificial dielectric layer which was subsequently etched away. The bridge is robust enough to stand up to wafer cleaving to leave the free-standing YBCO line seen in the scanning electron microscope (SEM) picture. As illustrated in Fig. 2, the sequence of steps illustrating formation of YBCO air bridges are the following: after the substrates are cleaned by ultrasonic agitation in acetone and blow dried by clean dry nitrogen gas, we deposit 300–400 nm of epitaxial  $\text{SrTiO}_3$  as a sacrificial dielectric layer on a  $\text{LaAlO}_3$  substrate. The  $\text{SrTiO}_3$  is then patterned with conventional photolithographic techniques using AZ 4620

photoresist, Ar ion milling, and acetone resist stripping to form the region of YBCO to be free standing (suspended). The surface of the remaining  $\text{SrTiO}_3$  regions are 300–400 nm above the surrounding bare substrate regions, requiring the subsequently deposited YBCO to traverse a 300–400 nm step. In order to provide a high-quality epitaxial layer of YBCO across this step, we control the slope of the edge of the  $\text{SrTiO}_3$  regions by dry etching with an ion mill. Dry etching techniques are more reproducible than wet chemical etching processes and, in particular, ion beam etching can make smooth and controlled angles for the steps at the edges of the  $\text{SrTiO}_3$  regions. For the air bridge itself, we deposit 300–500 nm of YBCO. After masking with photoresist to define the extent of the superconducting regions of the final device, we then dry etch this YBCO layer. To convert the  $\text{SrTiO}_3$  supported air bridge into a free-standing suspended structure, we selectively wet etch the  $\text{SrTiO}_3$  using a weak HF solution. Previous wet etching tests indicated that the etching rate for  $\text{SrTiO}_3$  is approximately 1  $\mu\text{m}/\text{min}$  under gentle ultrasonic agitation in a room temperature solution of 25% HF in water. Similar wet etch tests on thin film layers of YBCO deposited by laser ablation indicated an etching rate of about 4 nm/min. Thus, for properly designed structures, there is no need to passivate the YBCO during this  $\text{SrTiO}_3$  wet etching process.

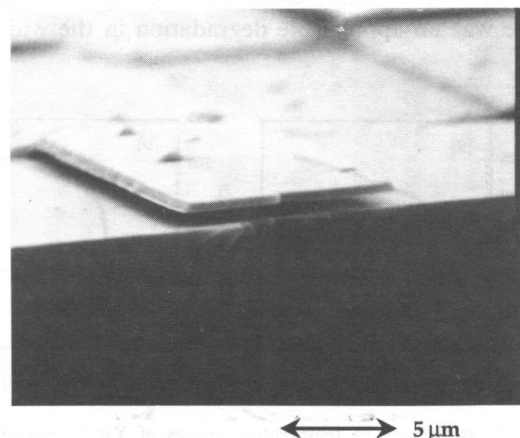


FIG. 1. SEM microphotograph of the YBCO air bridge.

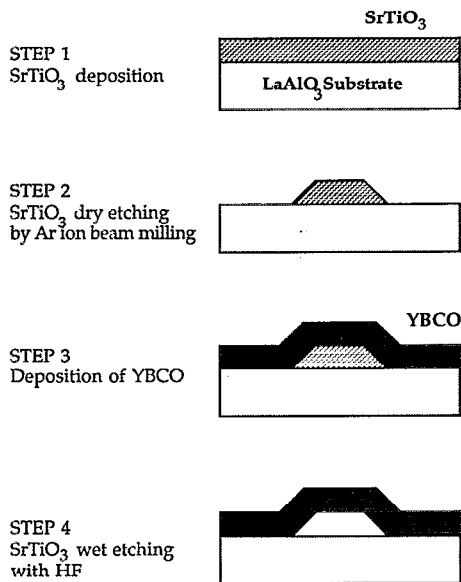


FIG. 2. Sequence of steps illustrating formation of YBCO air bridge.

The superconducting properties of the YBCO were examined to identify any possible degradation from the above processing steps. For the electronic transport measurements, the samples were mounted on a temperature-controlled copper sample platform which was inserted into a liquid helium dewar above the liquid helium level. Although the temperature of the copper sample platform was controlled by a commercial temperature controller to within 10 mK, the samples were open to the colder helium gas. Thus, if the thermal conductance of the suspended air bridges is sufficiently low, the center portion of the air bridges should be below the temperature of the copper sample holder and the sample substrate. In Fig. 3(a) we show the resistance vs temperature curve for an air bridge before the sacrificial SrTiO<sub>3</sub> was removed. For this sample, the YBCO air bridge was  $\sim 300$ -nm thick,  $10$ - $\mu$ m wide and after the removal of the SrTiO<sub>3</sub> sacrificial layer the suspended portion was  $50$ - $\mu$ m long. The figure shows a transition at  $87$  K with a width of about  $1$  K. In Fig. 3(b) we show the resistance vs temperature for the same sample as in Fig. 3(a) after removal of the SrTiO<sub>3</sub> sacrificial layer. As can be seen from a comparison of Figs. 3(a) and 3(b), there was no appreciable degradation in the width of the

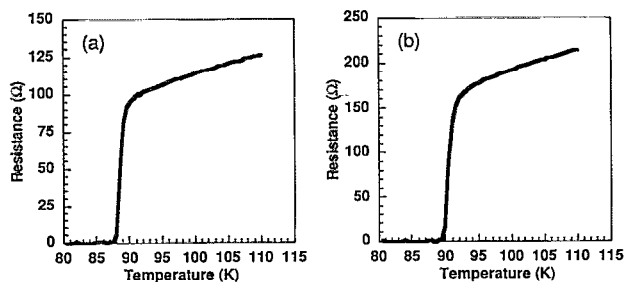


FIG. 3. Resistance vs temperature curves of YBCO microbridge (a) before the HF wet etch of the SrTiO<sub>3</sub> sacrificial layer (b) after the HF wet etch of the SrTiO<sub>3</sub> sacrificial layer.

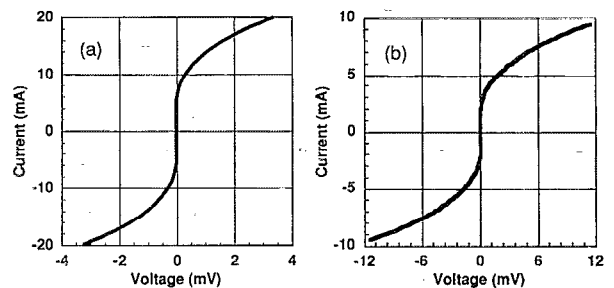


FIG. 4. Current vs voltage curves of the YBCO microbridge at  $77$  K (a) before the HF wet etch of the SrTiO<sub>3</sub> sacrificial layer (b) after the HF wet etch of the SrTiO<sub>3</sub> sacrificial layer.

superconducting transition by the SrTiO<sub>3</sub> removal process. As can also be seen by comparison of Figs. 3(a) and 3(b), the air bridge, once suspended, was cooled by the helium gas to about  $3^\circ$  below the temperature of the substrate. Thus its superconducting transition occurred when the copper sample platform and substrate were at  $90$  K. Since these photolithographically defined YBCO air bridges can be thermally decoupled from the underlying substrate, it should be possible to create monolithic YBCO bolometer arrays on a single substrate using standard photolithography techniques.

In Fig. 4 we show  $I$ - $V$  curves for the air bridge shown in Fig. 3 when the copper sample platform was held at  $77$  K. The critical current of the air bridge before it was suspended was  $5$  mA at  $77$  K [Fig. 4(a)]. This corresponds to a critical current density of  $\sim 1.3 \times 10^5$  A/cm<sup>2</sup>. This reduced current density may indicate that "step edge" junctions formed at the edges of the SrTiO<sub>3</sub> sacrificial layer.<sup>5</sup> After the SrTiO<sub>3</sub> etch process to suspend the air bridge, the critical current was  $3$  mA while the sample platform was held at  $77$  K [Fig. 4(b)]. The SrTiO<sub>3</sub> etch which produced this sample was  $2$  min long to accommodate the etching of some larger structures on the same chip set. Although the etch rate of the YBCO is considerably slower than the etch rate for SrTiO<sub>3</sub> ( $0.004$   $\mu$ m/min vs  $1$   $\mu$ m/min), the YBCO was reduced  $\sim 0.008$   $\mu$ m in width. Since both the top and the underside of the air bridge are exposed to the HF solution, the YBCO was reduced  $8$ – $16$  nm in thickness. Thus its cross-sectional area was reduced from  $4$  to  $\sim 3.8$   $\mu$ m<sup>2</sup>. This reduction in cross-sectional area should have caused a reduction in critical current of  $\sim 0.25$  mA, from  $5$  to  $\sim 4.75$  mA. An examination of the air bridges using SEM (Fig. 1) did not show any obvious cracks or constrictions. The fact that the observed reduction in critical current was a factor of  $8$  larger ( $\sim 2$  mA) might indicate that the region which produced the before-etch depressed critical current was more sensitive to the etching process than the rest of the YBCO. For example, it would not be unreasonable for the YBCO etch rate to be enhanced somewhat at the edges of the SrTiO<sub>3</sub> layer due to the large localized stresses. Nevertheless, Figs. 3 and 4 indicate that free-standing YBCO structures can be fabricated without a large degree of degradation in the intrinsic superconducting properties. Techniques for suppression of the grain

boundary nucleation at the SrTiO<sub>3</sub> steps are presently being studied.

In conclusion, we have successfully fabricated the first YBCO air bridge thus demonstrating a suspended HTS microstructure capable of being exploited for future device applications. These air bridges can be fabricated on LaAlO<sub>3</sub>, buffered sapphire or YSZ.<sup>2</sup> Although many of the mechanical properties of HTS oxides films are not known, we have shown a general approach to making suspended HTS structures analogous with that found in silicon mi-

crocircuit technology. This opens the possibility for numerous HTS applications in sensors and micromachines.

- <sup>1</sup>R. T. Howe and R. S. Muller, *Sensors and Actuators* **4**, 447 (1983).
- <sup>2</sup>L. P. Lee, K. Char, M. S. Colclough, and G. Zaharchuk, *Appl. Phys. Lett.* **59**, 3051 (1991).
- <sup>3</sup>D. B. Rutledge, D. P. Neikirk, and D. P. Kasilingham, *Infrared and Millimeter Wave* (Academic, New York, 1983), Vol. 10, Chap. 1.
- <sup>4</sup>W. Eidelloth, W. J. Gallagher, R. P. Robertazzi, R. H. Koch, and B. Oh, *Appl. Phys. Lett.* **59**, 1257 (1991).
- <sup>5</sup>K. P. Daly, W. D. Dozier, J. F. Burch, S. B. Coons, R. Hu, C. E. Platt, and R. W. Simon, *Appl. Phys. Lett.* **58**, 543 (1991).